

Multi-criteria protection scheme for online element failure detection in shunt capacitor banks

Goodarzi, Ali; Allahbakhshi, Mehdi ; Tajdinian, Mohsen ; Popov, Marjan

DOI

[10.1049/iet-gtd.2020.0347](https://doi.org/10.1049/iet-gtd.2020.0347)

Publication date

2020

Document Version

Accepted author manuscript

Published in

IET Generation, Transmission and Distribution

Citation (APA)

Goodarzi, A., Allahbakhshi, M., Tajdinian, M., & Popov, M. (2020). Multi-criteria protection scheme for online element failure detection in shunt capacitor banks. *IET Generation, Transmission and Distribution*, 14(19), 4152-4163. <https://doi.org/10.1049/iet-gtd.2020.0347>

Important note

To cite this publication, please use the final published version (if applicable). Please check the document version above.

Copyright

Other than for strictly personal use, it is not permitted to download, forward or distribute the text or part of it, without the consent of the author(s) and/or copyright holder(s), unless the work is under an open content license such as Creative Commons.

Takedown policy

Please contact us and provide details if you believe this document breaches copyrights. We will remove access to the work immediately and investigate your claim.

Multi-Criteria Protection Scheme for Online Element Failure Detection in Shunt Capacitor Banks

Ali Goodarzi¹, Mehdi Allahbakhshi^{1*}, Mohsen Tajdinian¹ and Marjan Popov²

1-School of electrical and computer engineering, Shiraz university, Shiraz, Iran

2- Delft University of Technology, Faculty of EEMCS, Mekelweg 4, 2628 CD, Delft, Netherlands

*Corresponding email: allahbakhshi@shirazu.ac.ir

Abstract: This paper deals with a fault detection investigation of SCBs, and it is focused on the faulty phase detection and the number of faulty capacitor units. Unlike previous methods, the proposed method provides a relay decision making criterion which determine the faulty capacitors, and the number of capacitor failures in case of multiple faulty phase conditions. The proposed algorithm is applied on different wye configurations of SCBs considering different protection designs (i.e., fuseless, internally and externally fused units). Since the detection of capacitor failures in SCBs are based on the fundamental phasor component, there may occur a significant delay in decision making in the case of an external short circuit fault in the power system. The aforementioned condition, which will be mathematically proven, happens due to a capacitor discharge after fault clearance. To deal with this condition, a method is proposed by applying an algorithm, in which the fundamental component of the voltage signal is extracted in one cycle. Performance evaluations associated with the proposed method are provided for different fault conditions, fault locations, and different levels of harmonics and, they are further discussed through the implementation of the proposed method in MATLAB environment.

1. Introduction

Capacitor units, which are widely employed in power system high voltage applications, are designed by utilizing different fuse-based protection technologies, which can be externally fused, internally fused, or even fuseless. It has been reported that the internally fused and fuseless technologies attract more interest for substation applications as a result of providing appropriate reliability and also fewer cost issues regarding the life cycle [1], [2]. Comparing to the externally fused technology of capacitor units, fuseless and internally fused technologies have higher accessibilities. However, last two technologies confront the disadvantage of having problems in identifying failed units due to lack of external fuses. As discussed in [3], system imbalance has become a major occurrence in power systems, and as a result, protection and control systems provided for Shunt Capacitor Banks (SCBs) require enhanced algorithms that are able to detect the faulty phases and units of SCBs. The aforementioned enhanced algorithms will help in faster localization of the faulty phases and units and thus, making the repair and preparation procedure of the SCBs for operation quicker. Also, these algorithms can be helpful for condition monitoring of the SCB capacitor units and consequently can result in the reduction of unscheduled outages of SCBs. It must be mentioned that except for some protection schemes that employ per-phase measurements [1], [5] - [7], the conventional unbalance protection functions confront challenges regarding localization of faulty points in SCBs, due to lack of an adequate number of available measurements [4].

By investigation of previously published papers regarding SCBs fault detection, location, and online monitoring focusing on unbalanced protection schemes, it is found that very few research studies have been conducted in this area. Generally, previously published methods are grouped into two categories. The first group of methods are designed for double wye configuration of SCBs and perform

their calculations based on the current measured at the neutral point [8] - [11]. These methods can detect the faulty phase and also the number of failed capacitor units using current-base unbalance relaying. A comprehensive review regarding unbalance protection schemes of double-wye SCBs can be found in [9].

The second group, which is the main interest of this paper, concentrates on the single wye configuration of SCBs and is based on the voltage of the neutral point [12]–[14]. As mentioned in [15], the calculations of these methods are conducted based on the reference of the phase angle of the neutral point from the phase angle of the positive sequence bus voltage. Through this selection of reference angle, the effects of negative sequence voltages on the phase angles of the phase voltages are disregarded. In [16], a method based on the negative sequence current has been proposed for the fault location in the single wye SCB configuration that solves the aforementioned problem regarding negligence of the contribution of the negative sequence in the referenced phase angle. The most recent protection scheme has been proposed in [4], which is based on Superimposed Reactance (SR). The application of the SR method is done by utilizing available voltages for an unbalance protection relay.

It should be noted that through surveying the literature, it is indicated that the research publications mostly focus on the application of the SCBs for the power quality improvement, reactive power management, and voltage stability improvement of the power system through optimal allocation of SCBs in the planning stage [17-22].

By considering the criteria given in [4], even though the SR method seems very comprehensive, some issues have neither been investigated nor addressed. These issues are mainly related to the performance of the protection scheme in case of multiple faulty units at the same time in different phases, the impact of the power system transient faults on delay time of the relay operation and the impact of harmonic pollution.

This paper presents an enhanced indicator for element failure detection that essentially calculates the per unit variations of the capacitor. The presented method, which is applied for each phase separately, utilizes only the available voltages of the unbalance protection relay. Similar to [4], the proposed method utilizes the fundamental phasor components for the determination of the fault location, without making use of the reference phase angle. The contributions of the paper are as follows:

- In addition to fault location identification, the proposed method utilizes some uncomplicated calculations to detect and determine the number of faulty units, as well. The criterion provided by the proposed method, contrary to [4], is also capable of detecting and determining the number of faulty units. The latter criterion is reflected in the newly developed calibrating factors, which are based on the new definition of k-factors and the unbalance relay input voltages. The new calibrating factors are able to discriminate the capacitor units' failures that may simultaneously or with sub-cycle delays occur by phase.
- The proposed algorithm, being developed considering different SCB wye configurations, can greatly ease the monitoring of the capacitor units, regardless of the protection design (i.e., fuseless, internally, and externally fused units).
- The other concerns regarding the capacitor failure detection in the SCBs comprise the issue that the numerical protection calculations are usually based on the fundamental phasor component. As a result, significant delays in decision making may occur in case of an external short circuit fault in the power system. In this paper, firstly, the behavior of the SCBs is investigated during a fault. Thereafter, to deal with the impact of the capacitor discharge behavior of the SCBs after fault clearance on the SCBs' protection scheme, the proposed protection scheme is provided a developed algorithm, in which the fundamental component of the voltage signal is extracted in one cycle. This extra algorithm helps preventing the undesired delay time in the relay trip signal of the SCBs.

The rest of the paper is organized as follows: the proposed methods and fundamental formulations are discussed in section 2. Section 3 presents the implementation procedure of the proposed method. Performance evaluation and meaningful conclusions are given in sections 4 and 5, respectively.

2. Problem statement and proposed algorithm

As previously discussed, the unbalanced protection scheme is the most important and vital protection of the SCBs against internal faults. In the following, the proposed protection scheme for identifying the faulty phase(s) and determining the number of failed units is presented for different SCB configurations. Different SCB configurations as illustrated in Fig. 1, are adopted from IEEE Std C37.99 [23]. It should be noted that the proposed algorithm is generally based on the fundamental phasor component of the neutral point voltage. As a result, the computation of the fundamental phasor component is realized by applying full cycle discrete Fourier transform (DFT).

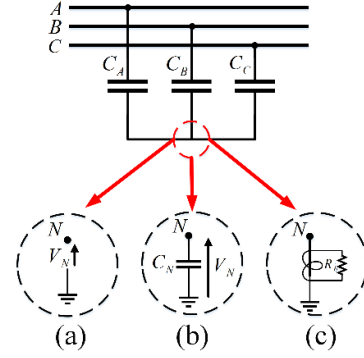


Fig.1. Different SCB configurations, (a) Ungrounded wye connection, (b) Ungrounded wye connection through a grounding capacitor at the neutral point, (c) Ungrounded wye connection through a low ratio current transformer

2.1. Calculation of k-factors

Fig.1.a shows the SCB configuration with an ungrounded wye connection (Con1). V_N , $V_{A,B,C}$, and $C_{A,B,C}$ correspond to the neutral point voltage, phase to ground voltages regarding each phase and the capacitor regarding each phase, respectively. Assuming the steady-state condition, by applying Kirchhoff's Current Law (KCL) at the neutral point, the following is concluded:

$$\frac{V_N - V_A}{-j\omega C_A} + \frac{V_N - V_B}{-j\omega C_B} + \frac{V_N - V_C}{-j\omega C_C} = 0 \quad (1)$$

$$\Rightarrow (C_A + C_B + C_C)V_N = C_A V_A + C_B V_B + C_C V_C$$

Two k-factors are defined as follows:

$$K_A \triangleq \frac{C_A}{C_C} \quad (2.a)$$

$$K_B \triangleq \frac{C_B}{C_C} \quad (2.b)$$

According to (2), expression (1) can be rewritten as follows:

$$(1 + K_A + K_B)V_N = K_A V_A + K_B V_B + V_C \quad (3)$$

By transforming (3) into a matrix form, the k-factors can be expressed as follows:

$$\begin{bmatrix} K_A \\ K_B \end{bmatrix} = \begin{bmatrix} V_A^{re} - V_N^{re} & V_B^{re} - V_N^{re} \\ V_A^{im} - V_N^{im} & V_B^{im} - V_N^{im} \end{bmatrix}^{-1} \begin{bmatrix} V_N^{re} - V_C^{re} \\ V_N^{im} - V_C^{im} \end{bmatrix} \quad (4)$$

where superscripts *re* and *im* correspond to the real, and the imaginary parts of the voltage phasor component.

The k-factors for ungrounded wye connection through a grounding capacitor at the neutral point (Con2) and ungrounded wye connection through a low ratio current transformer (Con3) are calculated as follows:

$$\begin{bmatrix} K_A \\ K_B \end{bmatrix} = \begin{bmatrix} V_A^{re} - V_N^{re} & V_B^{re} - V_N^{re} \\ V_A^{im} - V_N^{im} & V_B^{im} - V_N^{im} \end{bmatrix}^{-1} \begin{bmatrix} V_N^{re}(1 + K_N) - V_C^{re} \\ V_N^{im}(1 + K_N) - V_C^{im} \end{bmatrix} \quad (5)$$

$$\begin{bmatrix} K_A \\ K_B \end{bmatrix} = \begin{bmatrix} V_A^{re} - V_N^{re} & V_B^{re} - V_N^{re} \\ V_A^{im} - V_N^{im} & V_B^{im} - V_N^{im} \end{bmatrix}^{-1} \begin{bmatrix} V_N^{re}(1 + K_{CT}) - V_C^{re} \\ V_N^{im}(1 + K_{CT}) - V_C^{im} \end{bmatrix} \quad (6)$$

where K_N , and K_{CT} are expressed as follows:

$$K_N = \frac{C_N}{C_C} \quad (7.a)$$

$$K_{CT} = \frac{-j}{C_C * 2\pi f * CTR^2 * R_b} \quad (7.b)$$

It should be noted that, C_N is assumed to be about 10% of C_C [24]. It should be mentioned that besides the cost issue, the greater neutral capacitor will increase the stored energy, and consequently enhances the chance of damage to the connected measuring devices. Note that the lower neutral capacitor will increase the noise level. It is also worth noting that the different values of C_N do not impact the formulation or the procedure of the capacitor unit failure detection method. The variations of C_C , even due to capacitor unit failure are negligible, as a result, K_N is assumed to have a constant value.

2.2. Faulty phase identification criteria

In the previous sub-section, the k-factors regarding different configurations of SCBs were introduced. However, it should be mentioned that regardless of SCB configurations, they may benefit from a fuse protection scheme, resulting in various conditions associated with the identification of faulty phases. To provide some criteria for identifying faulty phases of SCBs, some assumptions are used, which are described as follows:

- Firstly, it is assumed that the capacitor failures will not occur simultaneously in all three phases. It should be mentioned that the scheme presented in [23], has also made this assumption in the calculations. However, it is worth mentioning that unlike [4], the proposed method can identify multiple capacitor unit failures in the case of two faulty phases.
- The second assumption in this algorithm is regarding the internal fuse configuration of SCB. It is assumed that the capacitor is decreased after the operation of the fuse. While in fuseless SCBs, after fault occurrence, the capacitor is increased. In SCBs with external fuse configuration, the capacitor of the SCB is increased in each phase at first, but after external fuse operation, the equivalent capacitor is decreased.

Based on the above-mentioned assumptions, the fault detection algorithms for different fuse protections of SCBs are given in Tables 1 and 2.

2.3. Determining the number of failed elements in each phase of the SCB

The number of failed elements is determined based on the variations of the total capacitance elements, before and after the internal fault, and the failed elements in each phase of the SCB. N_e denotes the total number of elements for the SCBs in each phase, during healthy condition. Considering Q_e as the reactive power of each element, the reactive power of the SCB in each phase before element failure (Q_{old}) and after element failure (Q_{new}) are calculated as follows:

$$Q_{old} = C_{old} V_{old}^2 \approx N_e^{old} * Q_e \quad (8.a)$$

$$Q_{new} = C_{new} V_{new}^2 \approx N_e^{new} * Q_e \quad (8.b)$$

In (8.a) and (8.b), it is assumed that the average value of reactive power after element failure occurrence remains

close to its nominal value. As a result, the number of failed elements (N_d) is calculated as follows:

$$\frac{C_{new}}{C_{old}} = \frac{N_e^{new}}{N_e^{old}} * \left(\frac{V_{old}}{V_{new}} \right)^2 \quad (9.a)$$

$$\Rightarrow N_d = N_e^{old} - N_e^{new} = \left(1 - \frac{N_e^{new}}{N_e^{old}} * \left(\frac{V_{old}}{V_{new}} \right)^2 \right) N_e^{old}$$

$$N_e^{new} = N_e^{old} - N_d \quad (9.b)$$

$$N_e = N_s * N_p * N_{us} * N_{up} * N_{br} \quad (9.c)$$

where N_d is the number of failed elements, N_s is the number of series sections in each unit, N_p is the number of parallel elements in each series section of each unit, N_{us} is the number of series sections of each capacitor unit per branch in each phase, N_{up} is the number of parallel units in each series section of units, and N_{br} is the number of unit branches in each phase. The superscripts *old* and *new* denote the status before and after the internal fault.

2.4. Temporary external short circuit fault effect on SCBs

Most of the suggested and concluded expressions in the previous subsections and also previous related published methods [4] are based on the fundamental phasor component of the voltage signal. DFT is one of the most famous phasor estimation algorithms that is widely utilized in digital relays for the calculation of the fundamental phasor component. However, as discussed in [25], there are several issues that could result in the inaccuracy of DFT due to the nature of the signal. The inaccuracy in calculation of the DFT will be reflected in the fundamental phasor component and may result in the addition of an unwanted delay or even maloperation of the digital relays. As a result, it is obvious that the phasor estimator should be equipped with proper auxiliary filters for dealing with disturbing transient components being generated from abnormal operating conditions.

Temporary external unbalanced short circuit faults may result in the generation of decaying transients in the neutral voltage of the SCBs. These transients definitely and profoundly affect the performance of the conventional DFT calculations. More importantly, such a situation may result in occurrence of overvoltages in other unfaultry phases, which may lead to single or multiple capacitor unit failure(s). As a result, it is vital to deal with the inaccuracy in the estimated fundamental component of the voltage. In the following, first, based on the superposition theorem in circuit analysis, the nature of the transients is mathematically modeled. After that, an auxiliary filter is introduced to enhance the immunity of the conventional DFT calculations to the aforementioned transients. Fig.2.a shows the schematic of a simple three phase power system containing an SCB. According to Fig.2.a, during a temporary fault condition, the capacitor unit and the inductance of the load may contain residual voltage and current components respectively. Obviously, these residual components get damped after some cycles. The neutral voltage waveform is generally expressed as follows:

Table1. K-factor conditions for identifying faulty phases regarding internal fuse protection of SCBs

Item	K-factors condition		Faulty phases	New capacitance value for faulty phases
1	$K_A^{new} > K_A^{old} \quad \& \quad K_B^{new} \leq K_B^{old}$		B,C	$\frac{C_c^{new}}{C_c^{old}} = \frac{K_B^{old}}{K_B^{new}}$ $\frac{C_a^{new}}{C_a^{old}} = \frac{K_B^{old}}{K_B^{new}} \times \frac{K_A^{new}}{K_A^{old}}$
2	$K_B^{new} > K_B^{old} \quad \& \quad K_A^{new} \leq K_A^{old}$		A,C	$\frac{C_c^{new}}{C_c^{old}} = \frac{K_A^{old}}{K_A^{new}}$ $\frac{C_b^{new}}{C_b^{old}} = \frac{K_A^{old}}{K_A^{new}} \times \frac{K_B^{new}}{K_B^{old}}$
3	$K_B^{new} > K_B^{old}$ $K_A^{new} > K_A^{old}$	$if \left\{ \left \frac{K_A^{old}}{K_A^{new}} - \frac{K_B^{old}}{K_B^{new}} \right < TR_1 \right\}$	C	$\frac{C_c^{new}}{C_c^{old}} = \frac{K_A^{old}}{K_A^{new}}$
4		$if \left\{ \frac{K_A^{old}}{K_A^{new}} < \frac{1}{TR_2} \times \frac{K_B^{old}}{K_B^{new}} \right\}$	B,C	Same as item 1
5		$if \left\{ \frac{K_B^{old}}{K_B^{new}} < \frac{1}{TR_2} \times \frac{K_A^{old}}{K_A^{new}} \right\}$	A,C	Same as item2
6	$K_A^{new} < K_A^{old} \quad \& \quad K_B^{new} = K_B^{old}$		A	$\frac{C_a^{new}}{C_a^{old}} = \frac{K_A^{new}}{K_A^{old}}$
7	$K_B^{new} < K_B^{old} \quad \& \quad K_A^{new} = K_A^{old}$		B	$\frac{C_b^{new}}{C_b^{old}} = \frac{K_B^{new}}{K_B^{old}}$
8	$K_B^{new} < K_B^{old} \quad \& \quad K_A^{new} < K_A^{old}$		A,B	$\frac{C_b^{new}}{C_b^{old}} = \frac{K_B^{new}}{K_B^{old}}$

Table2. K-factor conditions for identifying faulty phases in externally fused, and fuseless SCBs protection

Item	K-factors condition		Faulty phases	New capacitance value for faulty phases
1	$K_A^{new} < K_A^{old} \quad \& \quad K_B^{new} \geq K_B^{old}$		B,C	$\frac{C_c^{new}}{C_c^{old}} = \frac{K_B^{old}}{K_B^{new}}$ $\frac{C_a^{new}}{C_a^{old}} = \frac{K_B^{old}}{K_B^{new}} \times \frac{K_A^{new}}{K_A^{old}}$
2	$K_B^{new} < K_B^{old} \quad \& \quad K_A^{new} \geq K_A^{old}$		A,C	$\frac{C_c^{new}}{C_c^{old}} = \frac{K_A^{old}}{K_A^{new}}$ $\frac{C_b^{new}}{C_b^{old}} = \frac{K_A^{old}}{K_A^{new}} \times \frac{K_B^{new}}{K_B^{old}}$
3	$K_B^{new} < K_B^{old}$ $K_A^{new} < K_A^{old}$	$if \left\{ \left \frac{K_A^{old}}{K_A^{new}} - \frac{K_B^{old}}{K_B^{new}} \right < TR_1 \right\}$	C	$\frac{C_c^{new}}{C_c^{old}} = \frac{K_A^{old}}{K_A^{new}}$
4		$if \left\{ \frac{K_A^{old}}{K_A^{new}} > \frac{1}{TR_2} \times \frac{K_B^{old}}{K_B^{new}} \right\}$	B,C	Same as item 1
5		$if \left\{ \frac{K_B^{old}}{K_B^{new}} > \frac{1}{TR_2} \times \frac{K_A^{old}}{K_A^{new}} \right\}$	A,C	Same as item 2
6	$K_A^{new} > K_A^{old} \quad \& \quad K_B^{new} = K_B^{old}$		A	$\frac{C_a^{new}}{C_a^{old}} = \frac{K_A^{new}}{K_A^{old}}$
7	$K_B^{new} > K_B^{old} \quad \& \quad K_A^{new} = K_A^{old}$		B	$\frac{C_b^{new}}{C_b^{old}} = \frac{K_B^{new}}{K_B^{old}}$
8	$K_B^{new} > K_B^{old} \quad \& \quad K_A^{new} > K_A^{old}$		A,B	$\frac{C_b^{new}}{C_b^{old}} = \frac{K_B^{new}}{K_B^{old}}$

(Authors' version)

$$v_n(t) = v_{n,s}(t) + v_{n,cap}(t) + v_{n,ind}(t) \quad (10)$$

where $v_n(t)$, $v_{n,s}(t)$, $v_{n,cap}(t)$, and $v_{n,ind}(t)$ denote the total neutral voltage, the neutral voltage due to the voltage source, the neutral voltage due to capacitor residual voltage, and the neutral voltage due to inductance residual current, respectively.

In order to obtain a mathematical description for the effects of the source voltage, the inductance residual current and the capacitor residual voltage on the neutral voltage, utilizing the superposition theorem in circuit analysis, the following can be concluded.

2-4-1 The effect of voltage source on the neutral voltage

It is obvious that the general form of the neutral point voltage is similar to the voltage source. In other words, any harmonic component regarding the voltage source is reflected in the neutral point voltage waveform. As a result, the voltage waveform of the neutral point considering the voltage source effect is generally expressed as follows:

$$v_{n,s}(t) = \sum_{i=1}^h V_{n,i} \sin(2\pi fit + \theta_{n,i}) \quad (11)$$

where $V_{n,i}$, and $\theta_{n,i}$ are the magnitude, and the phase angle of the i -th harmonic component of the neutral voltage waveform. Also, f is the system frequency and it is equal to 50 Hz.

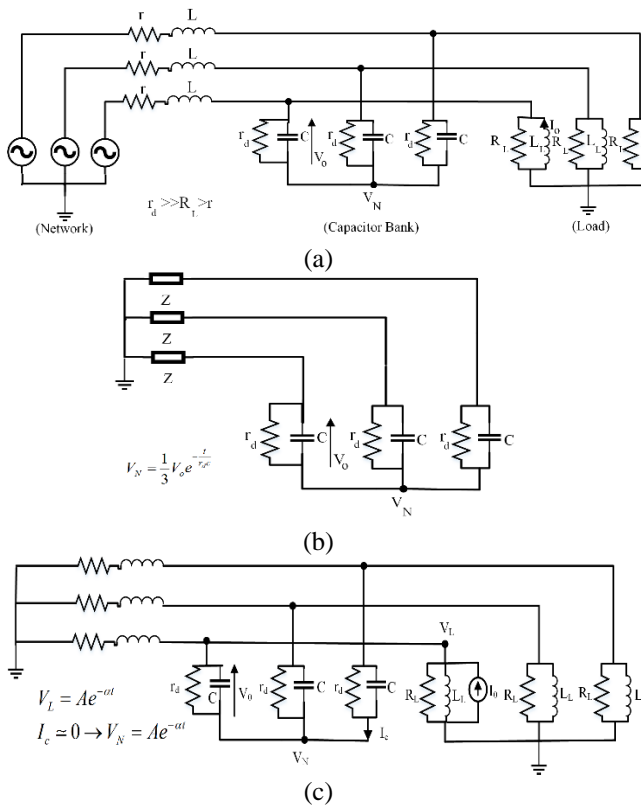


Fig.2. An illustration of a simple three phase power system with an SCB, (a) general illustration of the system, (b) the equivalent circuit for the effect of the capacitor residual voltage on the neutral voltage, (c) the equivalent circuit for

the effect of the inductance residual current on the neutral voltage

2-4-2 The effect of capacitor residual voltage on the neutral voltage

The equivalent circuit used to describe this condition is shown in Fig.2b. According to Fig.2b, the expression for $v_{n,cap}(t)$ can be obtained as:

$$v_{n,cap}(t) = V_{n,cap,0} e^{-t/\tau_c} \quad (12)$$

$$\tau_c = (r_d + (\frac{R_L \times r}{R_L + r}))C$$

where $V_{n,cap,0}$, τ_c , and C are the voltage magnitude at the neutral point due to the capacitor residual voltage, the circuit time constant, and the equivalent capacitor of the SCB for one phase. Also, r_d , R_L and r are the resistances regarding the SCB, the load, and the source respectively. According to [25], the value of R_s is much greater than r and R_L , and thus, τ_c is in order of minutes. Since the window length for the calculation of DFT is equal to one cycle (20 ms), $v_{n,cap}(t)$ can be approximately assumed a constant value during one cycle. Hence, the expression (12), can be rewritten as follows:

$$v_{n,cap}(t) = V_{n,cap,0} \quad (13)$$

2-4-3 The effect of inductance residual current on the neutral voltage

Similar to the previous discussion regarding the residual voltage of the capacitor, the equivalent circuit of the inductance residual current is shown in Fig.2. c. According to Fig.2.c, the expression for $v_{n,ind}(t)$ can be obtained as:

$$v_{n,ind}(t) = V_{n,ind,0} e^{-t/\tau_L} \quad (14)$$

$$\tau_L = \frac{(R_s + R_L)L}{R_s \times R_L}$$

where $V_{n,ind,0}$, τ_L , and L are the voltage magnitude at the neutral point due to load inductance residual current, the circuit time constant, and the load inductance for one phase.

Based on the above discussion and (10) to (14), the general form of the neutral voltage waveform is expressed as follows:

$$v_n(t) = V_{n,0} + V'_{n,0} e^{-at} + \sum_{i=1}^h V_{n,i} \sin(2\pi fit + \theta_{n,i}) \quad (15)$$

To remove the effect of DC terms, applying integration in (15) over one cycle, it can be written as follows:

(Authors' version)

$$\begin{aligned}
 X_1 &= \int_0^T v_n(t) dt \\
 &= \int_0^T (V_{n,0} + V'_{n,0} e^{-\alpha t} + \sum_{i=1}^h V_{n,i} \sin(2\pi f i t + \theta_{n,i})) dt \\
 &= \int_0^T V_{n,0} dt + \int_0^T V'_{n,0} e^{-\alpha t} dt + \int_0^T \sum_{i=1}^h V_{n,i} \sin(2\pi f i t + \theta_{n,i}) dt \quad (16) \\
 &= \int_0^T V_{n,0} dt + \int_0^T V'_{n,0} e^{-\alpha t} dt \\
 &= V_{n,0} T - \frac{V'_{n,0}}{\alpha} (e^{-\alpha T} - 1)
 \end{aligned}$$

By shifting the integration window by Δt and $2\Delta t$, and repeating (16), the following expressions are obtained:

$$X_2 = \int_{\Delta t}^{T+\Delta t} v_n(t) dt = V_{n,0} T - \frac{V'_{n,0}}{\alpha} (e^{-\alpha T} - 1) e^{-\alpha \Delta t} \quad (17)$$

$$X_3 = \int_{2\Delta t}^{T+2\Delta t} v_n(t) dt = V_{n,0} T - \frac{V'_{n,0}}{\alpha} (e^{-\alpha T} - 1) e^{-2\alpha \Delta t} \quad (18)$$

From (16) to (18), α , $V'_{n,0}$, and $V_{n,0}$ are calculated as follows:

$$\alpha = \frac{-1}{\Delta t} \ln\left(\frac{X_3 - X_2}{X_2 - X_1}\right) \quad (19)$$

$$V'_{n,0} = \frac{\alpha(X_2 - X_1)}{(e^{-\alpha T} - 1)(1 - e^{-\alpha \Delta t})} \quad (20)$$

$$V_{n,0} = \frac{1}{T} \left(X_1 + \frac{V'_{n,0}}{\alpha} (e^{-\alpha T} - 1) \right) \quad (21)$$

After calculating α , $V'_{n,0}$, and $V_{n,0}$, the DC terms can be removed from $v_n(t)$ as follows:

$$\begin{aligned}
 v_n^{new}(t) &= v_n(t) - (V_{n,0} + V'_{n,0} e^{-\alpha t}) \\
 &= \sum_{i=1}^h V_{n,i} \sin(2\pi f i t + \theta_{n,i}) \quad (22)
 \end{aligned}$$

In this stage, by applying DFT in (22), the fundamental phasor voltage component of the neutral point can be estimated without the unwanted effects of the DC terms.

3. Implementation

This section describes the implementation procedure of the proposed algorithm for capacitor element failure detection in the SCBs. In this paper, the test systems are implemented in PSCAD to obtain the signals required for the proposed algorithm, whilst the proposed algorithm is implemented in MATLAB.

The proposed method basically conducts its calculation based on the phasor component. The fundamental phasor component is calculated based on the discrete Fourier algorithm. Comparing the frequency range of the traveling wave, and the window length required for phasor calculation, the impact of very high-frequency is automatically ignored in the calculation. Even if the high-frequency components are

very impactful, the phasor calculation procedure is performed for consecutive windows of data (i.e. window length assumed 1 ms) so that the error of calculated phasor in two consecutive windows becomes less than 0.01%.

Depending on the SCB configuration, the neutral voltage and/or current signals are required as the input data of the proposed algorithm.

For each fault scenario, that is analyzed by the proposed algorithm, the following steps should be applied:

Step 1(Initialization): In this step, the requirements of the SCB model including the type of the SCB, the number of elements and units, and other information regarding the power network, being required for the simulation are entered in PSCAD based network.

Step 2(Simulation in PSACD): Using PSCAD simulation environment, the simulation is performed with a 1 μ s step time. For each time step of the simulation, the phase and the neutral voltage/current signals are transferred to MATLAB environment in order to perform the proposed algorithm.

Step 3(Phasor Calculation): Since the proposed method conducts its calculation based on the fundamental component, it is essential to calculate the fundamental phasor component from the signal. Therefore, by using (15) to (22), the fundamental voltage (or current) component is calculated. Note that the sampling rate required to apply the phasor calculation is adjusted to 100 μ s.

Step 4(K-Factor Calculation): Based on the phasor calculated in Step 3, the K-Factors are calculated using (4), (5) or (6).

Step 5(Prevent Negative Impact of Transients): Due to the unwanted impact, that may be imposed by transients during external faults, the calculated $K(t)$ is compared with the previous stage until the variation of $K(t)$ from two consequent steps of $K(t)$ (i.e. 100 μ s) becomes lower than α . Note that α is assumed 0.0001.

Step 6(Fault Location): Once $K(t)$ applies in the criterion of Step 5, the fault location is determined using the obtained $K(t)$. Note that the fault location is determined based on the expressions in Tables 1 and 2.

Step 7(NoFE Calculation): Based on the new value of capacitor, NoFE is calculated using (9).

Step 8(Updating K-Factors): Finally, K-factors are updated for the next simulation step time and the algorithm is repeated until the end of the simulation.

It should be noted that the Steps 1 and 2 are performed in PSCAD whilst the proposed algorithm is implemented in MATLAB environment.

4. Performance evaluation of the proposed method

To evaluate the performance of the proposed method, several case studies under different circumstances, and for different system grounding of SCBs are discussed. Several scenarios including consecutive element failures, simultaneous element failures in one phase and simultaneous element failures on multiple phases are observed. The test system shown in Fig.4 is utilized for the simulation of the cases, expect for the case of the capacitor bank with external fuse. All simulations are performed in PSCAD and MATLAB simulation environment. The specifications of the test system are given in Table 3.

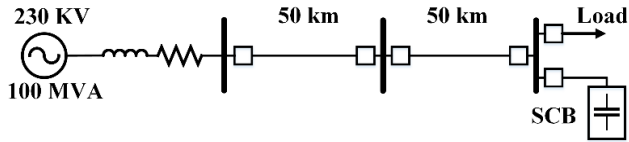


Fig.4. Single Line Diagram of the Test system

As it can be seen in Fig.4, the test system is provided with an SCB to study both the internally fused and the fuse-less configurations of the SCBs. The specifications of the desired SCB configurations are given in Table 4. It should be mentioned that the grounding systems in the configurations illustrated in Fig. 5 consist of isolated, solidly grounded, grounded with a capacitor, and grounded with CT.

Table3. Specifications of the test system given in Fig.4

Source Impedance	$Z_1 = 1.5 + j10, Z_0 = 15 + j30$
External Impedance	$5 + j5$
Balanced Load	120MW, 0.9Lag
Transmission Lines	$Z_1 = 25.45 \angle 85.9^\circ, Z_0 = 68.76 \angle 74.6^\circ$
Capacitor bank	70 MVAR

Table 4. The Specifications of the internally fused and the fuse-less SCBs

Bank type	S	P	U_s	U_p	br	$C_{element}$
Internal fuse	3	14	6	2	2	$1.36 \mu f$
fuse less	6	1	12	1	5	$60.8 \mu f$

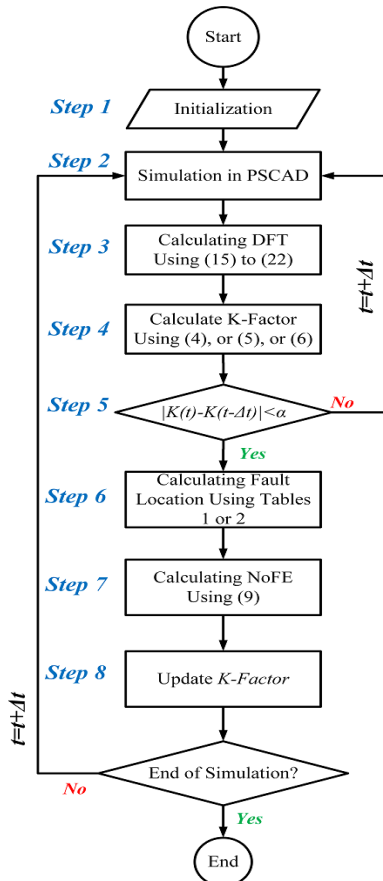


Fig.3. Implementation flowchart of the proposed algorithm

To show the capability of the proposed method, the monitoring of the desired parameters including the detection of the faulty phase, the estimation of the number of failed elements in the faulty phases and the determination of the failed capacitors in each phase is analysed for each time step of the simulation for all case studies.

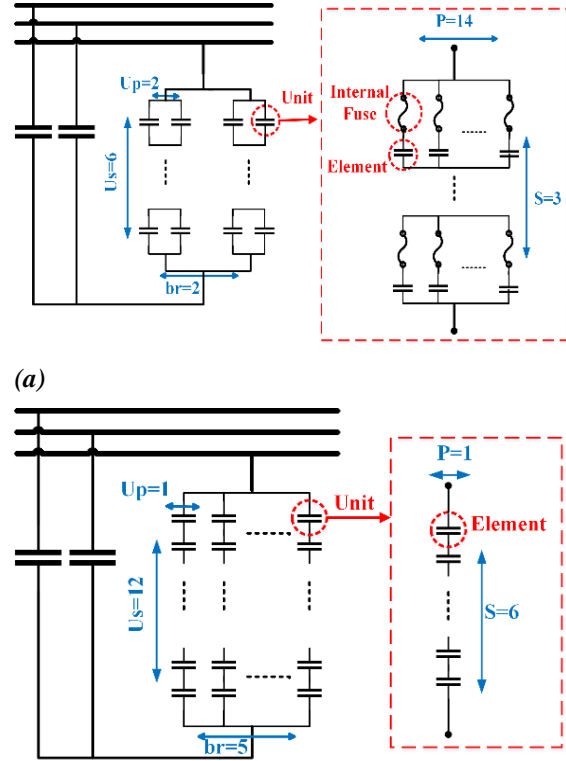


Fig.5. (a) An illustration of internally fused SCB, (b) An illustration of fuseless SCB

4.1. Star Connection SCBs with Ungrounded Neutrals

Table 5 shows the specifications for the fault scenarios regarding an internally fused ungrounded SCB. It should be noted that the fault scenarios are not necessarily in a specific unit and may be in different units, leading to excessive difficulty in SCB monitoring. To address the failed elements in an SCB, three parameters including FIT, FDT, NoFE are specified in the figures depicting the simulation results figures. These parameters are described as follows:

FIT (Fault Inception Time): The instant at which the fault is applied and a certain number of elements are shorted.

FDT (Fault Detection Time): The instant at which the proposed method successfully detects the failed elements.

NoFE (Number of Failed Element): This parameter is calculated based on (9) to show whether the calculated NoFE is equal to applied failures.

Table 5. specifications of the fault scenarios for an internally fused ungrounded SCB

FIT (s)	0.15	0.2	0.25	0.3	0.35	0.4	0.45
Phase A	1	1	0	1	0	2	0
Phase B	0	0	2	1	0	0	2
Phase C	2	0	0	0	2	1	1

(Authors' version)

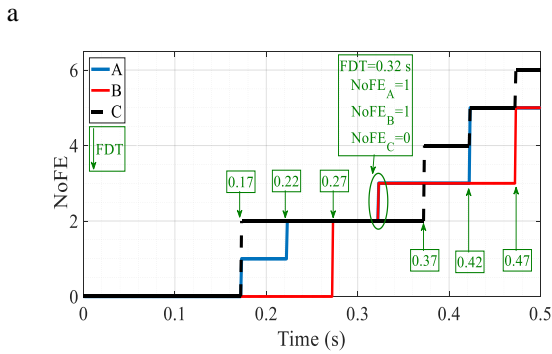
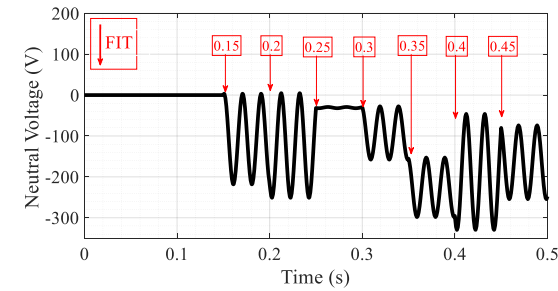


Fig.6. Performance of the proposed method in the case of an SCB with star connection and ungrounded neutral (a) Neutral voltage, (b) failed elements

Fig.6a shows neutral voltage signals regarding the scenarios given in Table 5. As it can be seen in Fig.6a, due to each unit failure specified in Table 5, the neutral voltage signal experiences different levels of variations. Fig.6a shows the capacitor element failures in an SCB. However, it is unclear how many elements are failed in each phase.

According to Fig.6b, the proposed algorithm detects the elements failed in each phase with almost one cycle delay. For instance, according to Table 5, the failure in the first scenario has occurred at $t=0.15$ s with the NoFE for phases A, B and C being 1, 0, 2, respectively. As can be seen in Fig.6b, the proposed algorithm detects the failed elements at $t=0.17$ s (with one cycle delay) and the NOFE calculated by the proposed method matches the quantities in Table 5. As illustrated in Fig.6b, the proposed method can track the element failures exactly as considered for each scenario by Table 5. From Fig.6b, it is obvious that the proposed method can detect the element failures, which are simultaneously occurred in two phases.

Also, as it can be seen in Fig.6a, that between 0.25 s and 0.3 s, the fundamental component of the neutral voltage signal has a zero value, however, according to Table 5, some elements are failed. As it can be seen in Fig.6b, the proposed method detects the element failures in phases A, B, and C; being in consistency with Table 5.

It is noteworthy that the zero value in Fig.6a will lead to maloperation of the SCB relay in element failure detection, and consequently, the maloperation of the CB [23]. However, the proposed algorithm can deal with the aforementioned issues with very good accuracy.

4.2. Star Connection of the SCB with Neutral Capacitor Grounding

The specifications of the element failure scenarios for an internally fused SCB with neutral capacitor grounding is provided in Table 6.

Table 6. Specifications of the fault in SCB

FIT (s)	0.15	0.2	0.3	0.35	0.4	0.45
Phase A	0	2	1	0	1	1
Phase B	2	0	1	1	0	2
Phase C	2	1	0	2	1	0

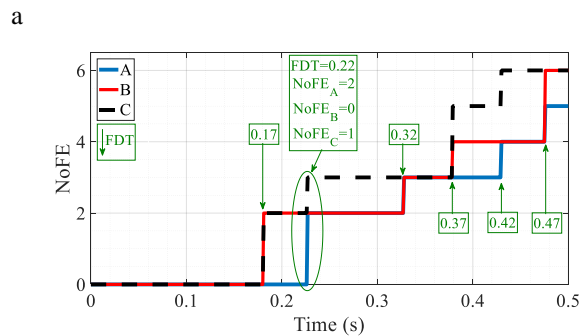
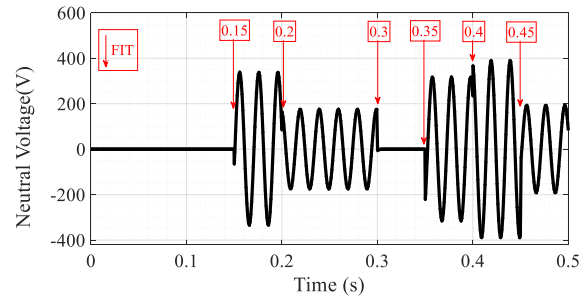


Fig.7. Performance of the proposed method in the case of a star connection SCB with neutral capacitor grounding (a) Neutral voltage, (b) failed elements

Same as the previous case study, different scenarios which are applied to the SCB are given in Table 6. The scenarios are designed to show the performance of the proposed algorithm in the case of simultaneous element failures in multiple phases.

Fig.7a shows the neutral voltage signal before and after applying the element failures to the SCB. As it can be seen in Fig.7b, the proposed method detects and tracks element failures very accurately and in agreement with Table 6. For instance, as illustrated in Fig.7b, the NoFEs for phases A, B, and C regarding the scenario being applied at $t=0.2$ match to the data in Table 6. Overall, just as the previous case study, it can be concluded that the proposed method can detect and monitor the condition of the capacitor grounded SCB during capacitor failures in the case of involving multiple phases simultaneously.

Table 8. The levels of imbalance and the injected harmonics in the applied voltage

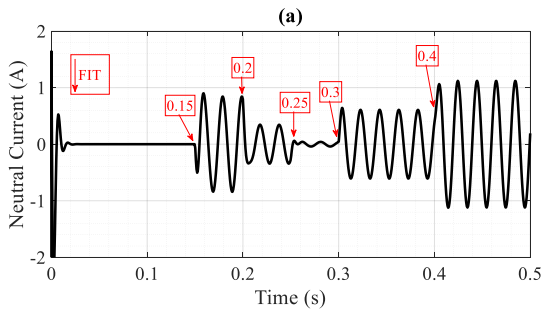
Phases	Fundamental component (kV)	5-th harmonic (% of fundamental component)	7-th harmonic (% of fundamental component)	11-th harmonic (% of fundamental component)
A	$230/\sqrt{3}\angle 10$	$0.35U_N\angle 10$	$0.2U_N\angle 80$	$0.07U_N\angle 45$
B	$253/\sqrt{3}\angle -150$	$0.18U_N\angle -32$	$0.12U_N\angle -59$	$0.09U_N\angle -142$
C	$207/\sqrt{3}\angle 100$	$0.24U_N\angle 165$	$0.04U_N\angle 56$	$0.06U_N\angle 48$

4.3. SCBs with Star Connection, and Neutral CT Grounding

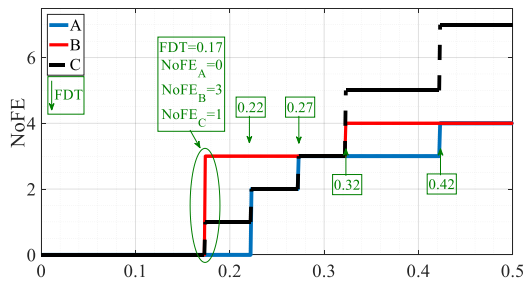
The specification of the fault scenarios for an internally fused SCB with neutral CT grounding is provided in Table 7. The selected CT in this study has a ratio of 50/5 and a 10-ohm burden [4].

Table 7. Specifications of the fault in CB

FIT (s)	0.15	0.2	0.25	0.3	0.4
Phase A	0	2	1	0	1
Phase B	3	0	0	1	0
Phase C	1	1	1	2	2



a



b

Fig. 8. Performance of the proposed method in the case of SCBs with star connection and neutral CT grounding (a) Neutral current, (b) failed elements

Fig. 8a illustrates the natural current regarding an SCB with CT grounding considering different element failure scenarios. As it can be seen in Fig. 8b, the proposed method precisely detects and tracks the failed elements in each

scenario with only one cycle delay with respect to the FITs shown in Table 7. As mentioned before, the proposed method operates based on the fundamental voltage component. It is obvious that the calculation of the fundamental voltage component with DFT is associated with one cycle delay. Note that in the case of neutral grounding with a CT, the neutral current signal is converted to a voltage signal and then is applied to the proposed method. Regarding

this case study, the proposed method is able to deal with simultaneous element failures in multiple phases.

4.4. Effects of harmonics and unbalanced voltages

Similar to subsection 4-1 to 4-3, the performance of the proposed method is investigated regarding a fuseless SCB with capacitor grounded under non-sinusoidal conditions. The specifications for the scenarios are given in Table 6. Moreover, the levels of imbalance and the injected harmonics in the applied voltage are tabulated in Table 8.

As it is clear in Fig. 9d, the proposed method tracks the correct number of element failures with one cycle delay. As a result, it can be concluded that the proposed method shows robust performance under harmonic polluted and imbalance voltage signal.

4.5. Effect of the power grid short circuit faults

In this section, the performance of the proposed method during short circuit faults in a power grid is investigated. In this situation, it can be expected that the neutral voltage or current experience a significant enhancement due to the decaying DC component. As a result, the monitoring algorithms falsely assume that several elements are failing.

To deal with this situation, a criterion is provided by the proposed algorithm, which suspends the procedure of updating the K-factors in case the neutral voltage suddenly rises up to 30% of the nominal voltage in each phase. This criterion, somehow acting as a short circuit detection method in the power grid, continues to suspend the K-factor calculations until the short circuit fault is cleared. After the fault clearance, K-factors will be updated using the pre-fault data to detect the potential element failure that may or may not have occurred during the short circuit fault in the power grid. For the sake of the simulations, a single-phase ground fault is started at $t=0.23$ s and removed at $t=0.28$ s. The specifications for studying element failure in an ungrounded internally fused SCB in the case of an external short circuit fault are provided in Table 9. As it can be seen in Fig. 10, the neutral voltage experiences a significant rise. After the fault clearance, the voltages of the different phases of the SCB are ought to be balanced. As a result, a transient unbalance overvoltage appears in the neutral of the SCB. After this transient overvoltage, the neutral voltage containing decaying DC components causes inaccuracy in estimation of the fundamental component using conventional DFT, as shown in Fig. 6b. Nevertheless, as it can be seen in Fig. 6c, using (15) to (22), the fundamental component of the neutral voltage signal can be appropriately calculated with maximum immunity to the decaying DC component.

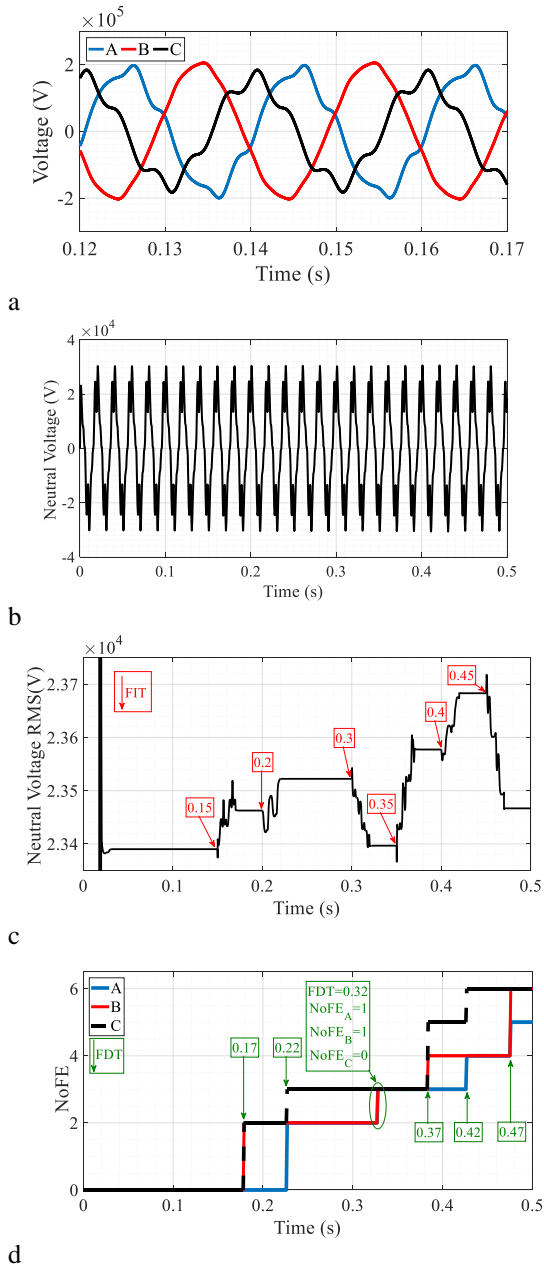


Fig.9. Performance of the proposed algorithm considering the effects of harmonics and unbalanced voltages (a) SCB phase voltages, (b) the neutral voltage, (c) RMS of the Fundamental harmonic of the neutral voltage, (d) failed elements.

Table 9. Specification of fault in SCB

FIT (s)	0.15	0.2	0.25	0.4	0.45
Phase A	1	1	1	2	0
Phase B	0	0	3	1	2
Phase C	2	0	0	0	1

4.6. Externally Fused Capacitor Banks

Consecutive element failures, which usually occur in SCBs with external fuses, will continuously occur until the fuse of the faulty unit melts [27]. In that case, an indication flag is raised, denoting the faulty unit [14]. A series of test

cases showing how the proposed method provides a fast and a reliable solution to avoid melting of the external fuses are provided in this section. It is also worth noting that similar to the fuseless SCB, when an element fails in an SCB with external fuse, it means that the element is short-circuited. To verify the performance of the proposed method for SCBs with external fuses, a test case is provided, as depicted in Fig.11. The specifications of the externally fused SCB and the scenarios considered through regarding case studies are given in Tables 10 and 11, respectively.

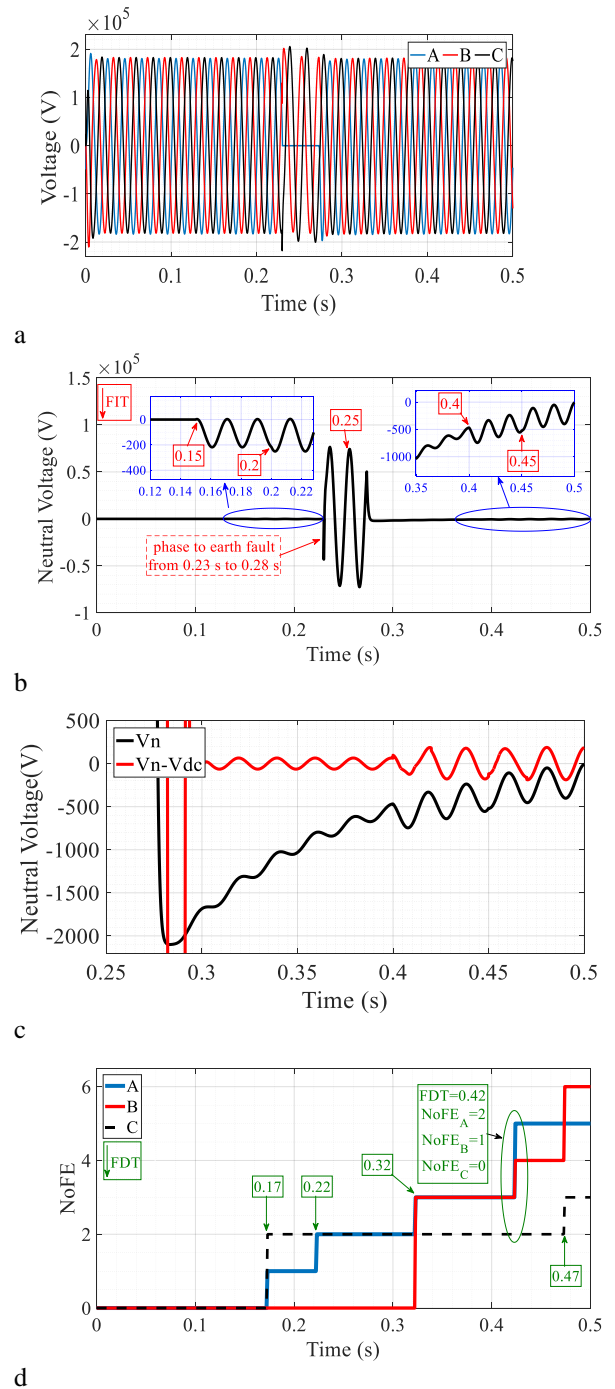


Fig.10. Performance of the proposed algorithm considering the effect of power grid short circuit faults (a) phase voltages of the SCB, (b) neutral voltage, (c) Fundamental harmonic of the neutral voltage with/without DC component (d) failed elements.

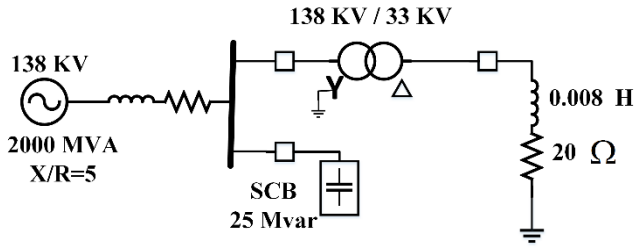


Fig.11. Test System for Verification of the Proposed Method Performance for an Externally Fused SCB

Table 10. Specification for the SCB with External Fuse

Bank type	S	P	U_s	U_p	br
External fuse	8	3	5	14	1

Table 11. Specification of Fault Scenarios for the Externally Fused SCB

FIT (s)	0.15	0.2	0.3
Phase A	0	4	1
Phase B	4	0	2
Phase C	2	4	0

Fig.12.a shows that the voltage signal of the neutral is changed after applying the scenarios. The performance of the proposed algorithm is shown in Fig.12b. As it can be seen in Fig.12b, the proposed method monitors the scenarios with high accuracy and total match to Table 11. Accordingly, the proposed method can overcome the challenges regarding this configuration of the SCBs.

4.7. Performance Comparison of the SCB Monitoring Algorithms

To evaluate the performance of the proposed algorithm, several SCB element failure scenarios were applied to the proposed failure detection method. The capabilities and the salient features (C&SF) of the proposed method and the previously published methods in SCB element failure detection are summarized in Table 12.

From Table 12, it can be observed that:

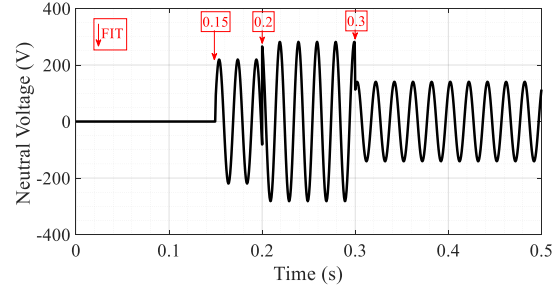
- All methods are able to detect the faulty phases.
- The proposed method and also the Methods in [4] possess the C&SFs 2 to 6 while the methods in [12], [13]

Table12. The capabilities and salient features of the proposed method and the state-of-the-arts

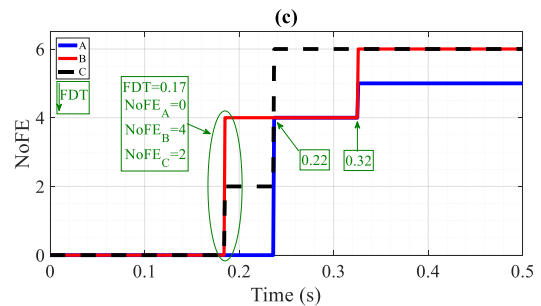
Number	C&SF	[16]	[12],[13]	[4]	Proposed method
1	Detecting faulty phases	✓	✓	✓	✓
2	Detecting consecutive failures in a single phase	✗	✗	✓	✓
3	Providing an Advanced criterion for fuse-saving of externally fused SCBs	✗	✗	✓	✓
4	Ability to deal with ambiguous failures	✗	✗	✓	✓
5	Applicable for different SCB configurations	✗	✗	✓	✓
6	Online Monitoring of the number of failed elements	✗	✗	✓	✓
7	Detecting the consecutive failures in two phases	✗	✗	✗	✓
8	Dealing with the decaying DC component	✗	✗	✗	✓
9	Robustness against voltage unbalance and harmonic polluted signals	✗	✗	✗	✓

and [16] are unable to respond correctly to these conditions.

C&SFs 7 to 9 are the unit C&SFs that only the proposed method can deal with them. No discussions have been given in the previously published algorithms regarding these C&SFs.



a



b

Fig.12. Performance of the proposed method for externally fused SCBs, (a) neutral voltage, (b) Number of failed elements in each phase

In order to compare the performance of the proposed algorithm with the previous published papers, performance evaluations are conducted between the proposed method and the methods proposed in [4] and [8] which are so far the most efficient algorithms. In this comparison, all six scenarios introduced in subsections 4.1 to 4.6 are applied to the suggested methods in [4] and [8]. The results are provided in Table 13. It should be noted that (X, Y, Z) shows the NoFE corresponding to each phase. The red font in Table 13 is representative for a failure in correct detection.

Table 13. Performance comparison between the proposed method and the methods presented in [4] and [8]

Scenarios	Algorithm	FIT (s)						
		0.15	0.2	0.25	0.3	0.35	0.4	0.45
4.1. According to the table 5	[4], [8]	(0,0,1)	(1,0,0)	(0,2,0)	(0,0,1)	(0,0,2)	(1,0,0)	(1,0,0)
	Proposed Method	(1,0,2)	(1,0,0)	(0,2,0)	(1,1,0)	(0,0,2)	(2,0,1)	(0,2,1)
4.2. According to the table 6	[4], [8]	(3,0,0)	(1,0,0)	(0,0,0)	(0,0,0)	(0,0,1)	(0,1,0)	(0,1,0)
	Proposed Method	(0,2,2)	(2,0,1)	(0,0,0)	(1,1,0)	(0,1,2)	(1,0,1)	(1,2,0)
4.3. According to the table 7	[4], [8]	(0,4,0)	(1,0,0)	(0,1,0)	(0,0,2)	(0,0,0)	(0,0,1)	(0,0,0)
	Proposed Method	(0,3,1)	(2,0,1)	(1,0,1)	(0,1,2)	(0,0,0)	(1,0,2)	(0,0,0)
4.4. According to the table 6	[4], [8]	(0,0,0)	(0,0,0)	(0,0,0)	(0,0,0)	(0,0,0)	(0,0,0)	(0,0,0)
	Proposed Method	(0,2,2)	(2,0,1)	(0,0,0)	(1,1,0)	(0,1,2)	(1,0,1)	(1,2,0)
4.5. According to the table 9	[4], [8]	(0,0,2)	(1,0,0)	(0,0,0)	(0,0,0)	(0,0,0)	(0,0,0)	(0,0,0)
	Proposed Method	(1,0,2)	(1,0,0)	(1,3,0)	(0,0,0)	(0,0,0)	(2,1,0)	(0,2,1)
4.6. According to the table 11	[4], [8]	(0,5,0)	(0,7,0)	(0,0,0)	(0,1,0)	(0,0,0)	(0,0,0)	(0,0,0)
	Proposed Method	(0,4,2)	(4,0,4)	(0,0,0)	(1,2,0)	(0,0,0)	(0,0,0)	(0,0,0)

As it can be seen in Table 13, the following is concluded:

- For scenarios 4.1 to 4.3 and 4.6, the proposed method successfully detects all failures, in contrast to the methods [4], [8] which failed to correctly detect NoFE. The reason of failure in [4] and [8] is that these methods can only deal with just one failure in one phase, whilst in the observed scenarios, multiple failures have occurred in several phases.
- In scenario 4.6, the suggested methods in [4] and [8] cannot deal with the level of voltage unbalance and also the harmonic levels are higher than permissible level. While the proposed method can successfully deal with any level of voltage unbalance and harmonic contents, even higher than permissible level, which may occur in case of using a static var compensators or harmonic filters.
- Eventually, since the methods in [4] and [8] cannot deal with the transients caused by capacitor discharge in fault voltage signals due to external fault conditions, these methods have failed in all cases. However, as it can be seen in Table 13, the proposed method has successfully dealt with this condition.

From Tables 12 and 13, it should be noted that the inclusion of C&SFs 7 to 9 made the proposed method more complex comparing to the state-of-the-art. However, the proposed method can deal with different challenges (i.e. the challenges in Table 12) of the element failure detection for various SCB configurations with promising accuracy and speed of convergence, comparing with existing methods.

5. Conclusion

Inability of having fast condition monitoring of the capacitor units, may results in extensive damage to the SCBs. In this paper, a new algorithm for online monitoring of the

SCBs is proposed that focuses on finding the faulty phase and the number of the failed capacitor units. Depending on the grounding systems of the SCBs, the proposed algorithm uses the fundamental component of the voltage or the current signal as an input parameter of the algorithm. The performance of the proposed algorithm was evaluated by different types of SCBs. By applying different types of fault scenarios for different types of SCBs, it can be concluded:

- The proposed method can be successfully used for capacitor unit failure detection in internally/externally fused and fuse-less configurations.
- The proposed method detects and calculates element failures within one cycle delay after a failure takes place.
- The decaying DC component leads to significantly large errors in the calculation of the fundamental component, which results in delayed decision making (i.e., more than one cycle delay.) The proposed method can deal with the decaying DC component due to external faults for protection of the SCBs; so that the decision making remains within almost one cycle.
- The proposed method can detect and calculate simultaneous element failures in different phases.

Simulation results also show that this algorithm can detect the element failures of SCBs, during simultaneous failures in multiple phases. As a result, it can be utilized for the protection of the SCBs.

While the proposed method has provided notable accuracy and fast response comparing to the state-of-the-art, it should be noted that due to phasor based calculation, the proposed method yet has one cycle delay in acquiring authenticated response. Therefore, more work should be done in order to reduce these time delays.

6. References

- [1] M. Dhillon and D. Tziouvaras, "Protection of fuseless shunt capacitor banks using digital relays," in 26th Annual Western Protective Relay Conference, October 1999.

(Authors' version)

- [2] Eaton's Cooper Power Systems catalog: Power capacitors, Cooper Power Systems, July 2014.
- [3] K. C. Agrawal, *Industrial Power Engineering and Applications Handbook*. MA, USA: Butterworth-Heinemann, 2001.
- [4] Jouybari-Moghaddam, H., et al. "New method of capacitors failure detection and location in shunt capacitor banks." 2018 71st Annual Conference for Protective Relay Engineers (CPRE). IEEE, 2018.
- [5] M. Bishop, T. Day, and A. Chaudhary, "A primer on capacitor bank protection," *Industry Applications, IEEE Transactions on*, vol. 37, no. 4, pp. 1174–1179, Jul 2001.
- [6] E. Price and R. Wolsey, "String current unbalance protection and faulted string identification for grounded-wye fuseless capacitor banks," in *65th Annual Georgia Tech Protective Relaying Conference*, May 2011.
- [7] Zhang, Ming, et al. "A shunt capacitor detection method based on intelligent substation." 2017 IEEE Conference on Energy Internet and Energy System Integration (EI2). IEEE, 2017.
- [8] Jouybari-Moghaddam, H., et al. "Enhanced Fault-Location Scheme for Double Wye Shunt Capacitor Banks." *IEEE Transactions on Power Delivery* 32.4 (2016): 1872-1880.
- [9] H. Jouybari-Moghaddam, T. S. Sidhu, M. R. Zadeh, and P. Parikh, "Enhanced fault location scheme for double wye shunt capacitor banks," *IEEE Transactions on Power Delivery*, vol. 32, no. 4, pp. 1872–1880, August 2017.
- [10] Z. Gajic, M. Ibrahim, and J. Wang, "Method and arrangement for an internal failure detection in a y-y connected capacitor bank," US Patent 20 130 328 569, December, 2013.
- [11] Ali, M. "Fault Analysis and Fault location in Fuseless split-wye shunt capacitor banks." 2019 International Symposium on Recent Advances in Electrical Engineering (RAEE). Vol. 4. IEEE, 2019.
- [12] S. Samineni, C. Labuschagne, J. Pope, and B. Kasztenny, "Fault location in shunt capacitor banks," in *Developments in Power System Protection (DPSP 2010). Managing the Change*, 10th IET International Conference on, March 2010, pp. 1–5.
- [13] J. Schaefer, S. Samineni, C. Labuschagne, S. Chase, and D. Hawaz, "Minimizing capacitor bank outage time through fault location," in *Protective Relay Engineers*, 2014 67th Annual Conference for, March 2014, pp. 72–83.
- [14] S. Samineni, C. Labuschagne, and J. Pope, "Principles of shunt capacitor bank application and protection," in *Protective Relay Engineers*, 2010 63rd Annual Conference for, March 2010, pp. 1–14.
- [15] B. Kasztenny, J. Schaefer, and E. Clark, "Fundamentals of adaptive protection of large capacitor banks - accurate methods for canceling inherent bank unbalances," in *Protective Relay Engineers*, 2007. 60th Annual Conference for, March 2007, pp. 126–157.
- [16] A. Kalyuzhny, J. C. McCall, and T. R. Day, "Corrective device protection," US Patent 7 973 537, July, 2011.
- [17] Abedini, Moein, Mahdi Davarpanah, Amir Sepehr, and Firouz Badrkhani Ajaei. "Shunt capacitor bank: Transient issues and analytical solutions." *International Journal of Electrical Power & Energy Systems* 120 (2020): 106025.
- [18] Machado, Alysson AP, Hélio MA Antunes, Igor A. Pires, Sidelmo M. Silva, and J. C. Braz Filho. "Probabilistic assessment and evaluation of transients in a medium voltage three-phase capacitor bank energized by unsynchronized vacuum switchgears." In *2016 IEEE Industry Applications Society Annual Meeting*, pp. 1-11. IEEE, 2016.
- [19] Gumilar, Langlang, Denis Eka Cahyani, Arif Nur Afandi, Dezetty Monika, and Stieven Netanel Rumokoy. "Optimization harmonic shunt passive filter using detuned reactor and capacitor bank to improvement power quality in hybrid power plant." In *AIP Conference Proceedings*, vol. 2217, no. 1, p. 030003. AIP Publishing LLC, 2020.
- [20] De Araujo, Leandro Ramos, Débora Rosana Ribeiro Penido, Sandoval Carneiro Jr, and José Luiz Rezende Pereira. "Optimal unbalanced capacitor placement in distribution systems for voltage control and energy losses minimization." *Electric Power Systems Research* 154 (2018): 110-121.
- [21] Sadeghian, Omid, Arman Oshnoei, Morteza Kheradmandi, and Behnam Mohammadi-Ivatloo. "Optimal placement of multi-period-based switched capacitor in radial distribution systems." *Computers & Electrical Engineering* 82 (2020): 106549.
- [22] Abdelsalam, Abdelazeem A., and Hany SE Mansour. "Optimal Allocation and Hourly Scheduling of Capacitor Banks Using Sine Cosine Algorithm for Maximizing Technical and Economic Benefits." *Electric Power Components and Systems* 47, no. 11-12 (2019): 1025-1039.
- [23] "IEEE Guide for the Protection of Shunt Capacitor Banks," *IEEE Std C37.99-2012 (Revision of IEEE Std C37.99-2000)*, pp. 1–151, March 2013.
- [24] C70 Capacitor Bank Protection and Control System, UR Series Instruction Manual, GE Digital Energy, November 2014.
- [25] Sidhu, T. S., et al. "Discrete-Fourier-transform-based technique for removal of decaying DC offset from phasor estimates." *IEE Proceedings-Generation, Transmission and Distribution* 150.6 (2003): 745-752.
- [26] IEEE Std 18- IEEE Standard for Shunt Power Capacitors, 2012, pp.5.
- [27] T. Ernst, "Fuseless capacitor bank protection," in *Proc. of Minnesota Power Systems Conf.*, 1999, pp. 77–83.